ferred from the few net-captured specimens. The obvious reason for this discrepancy between observations in situ and results from net hauls is the fragility of the houses (6), and perhaps that the unimposing preserved larvacean specimens are unrecognized in the gelatinous residues of net-haul samples.

ERIC G. BARHAM

Southwest Fisheries Center, National Marine Fisheries Service, National Oceanic and Atmospheric Administration, La Jolla, California 92038

References and Notes

1. R. W. Gilmer, *Science* **176**, 1239 (1972); W. H. Hamner, L. P. Madin, A. L. Alldredge, R. W. Gilmer, P. P. Hamner, *Limnol. Oceanogr.* **20**, 907 (1975).
2. A. L. Alldredge, *Science* **177**, 885 (1972); *Limnol. Oceanogr.* **21**, 14 (1976).
3. H. Lohmann, *Verh. Dtsch. Zool. Ges.* **19**, 200 (1909).
4. J. D. Trent, A. L. Shanks, M. W. Silver, *Limnol. Oceanogr.* **23**, 626 (1978); M. W. Silver, A. L. Shanks, J. D. Trent, *Science* **201**, 371 (1978).
5. C. Chun, *Aus den Tiefen des Weltmeeres* (Fischer, Jena, 1900), pp. 519–521.
6. C. P. Galt, *Fish. Bull*, in press.
7. As part of the U.S. Navy Electronics Laboratory deep submersible program, the major objective of my dives was acoustic scattering studies. Observations were also made when there was the opportunity, and some of these and early attempts to collect large larvacean houses have been discussed [E. G. Barham, *Oceans Mag.* **1**, 55 (1968)]. The submersible vehicles have been described [R. F. Busby, *Manned Submersibles* (Office of Oceanographer of the Navy, Washington, D.C., 1976)].
8. I thank I. E. Davies, a fellow observer on many dives, who first pointed out the similarity between textbook figures and the then unidentified structures. The work from *Deepstar 4000* was aided by pilots R. P. Bradley and R. Church, both now deceased. Discussions with C. P. Galt, A. L. Shanks, and J. D. Trent have been helpful. In late 1966, N. B. Marshall suggested in correspondence that the largest type house could be that of *Bathochordaeus charon*.

21 March 1979, revised 28 June 1979

The Viscous Sublayer at the Sea Floor

Abstract. *A 0.6-centimeter-thick sublayer was found in horizontal flow profiles obtained by traversing a heated thermistor from 19 centimeters above to 2 centimeters below the water-sediment interface in 200-meter-deep water on the Oregon continental shelf. In this sublayer the speed of the current varies linearly with distance above the sediment. Estimates of viscous stress from this sublayer and turbulent stress from the profile agree within 5 percent. Stress calculated from a current-meter spectrum agrees within its 95 percent confidence limits.*

Measurements of currents near the sea floor have been made for some years (*1*) but never within 1 cm of the bottom.

We present results from an experiment in which a heated thermistor was traversed over a 21-cm vertical travel, from 19 cm above the sediment-water interface to 2 cm below it. The site for the experiment lay in 199 m of water at 45°20.29′N, 124°20.34′W on the Oregon continental shelf. Grain size analysis of sediment in the area (*2*) indicates that the surface sediment is a silty sand (61 percent sand, 28 percent silt, and 10 percent clay). The mean diameter of a grain [computed by the method of Inman (*3*)] is 0.0042 cm. Time-lapse photographs taken by the motion-picture camera mounted on the instrument platform revealed no bedforms likely to significantly influence the flow.

The heated thermistor was tranversed by a crank-and-piston mechanism, which completed one cycle per minute. The signal was sampled every 1.5 seconds, together with the signal from an electrical potentiometer which indicated the position of the sensor. Because the drive was not linear, observations were not evenly spaced vertically, but the spacing was approximately 1.0 cm except near the top and bottom of the travel where it was less. The traversing velocity does not affect the results more than a few percent, because of the slowing of the drive near the boundary where the current is slow and because of the properties of the vector addition process. The thermistor was connected in a half-bridge configuration. Sufficient current was supplied to heat it to approximately 20°C above ambient temperature in typical flows. The sensing area of the thermistor was about 0.02 cm. Calibrations were performed by mounting the transducer on a whirling arm in a bath chilled to bottom-water temperatures. We have observed that the effect of pressure on these thermistors is negligible for these purposes at this depth; the effect of salinity also is not significant.

To construct a detailed profile from measurements spaced vertically 1 cm apart, a number of traverses had to be used to make up one profile. Sampling period and rotation period were incommensurate so samples eventually occurred at all vertical positions. This was an advantage in this case because waves (3.5 cm/sec orbital velocities, 15-second period) affected each profile so severely that averaging would have been required in any case; this way the wave motion was not coherent from one sample at a given height to the next nearby sample. The relative orientation of waves and the mean flow is not deducible from any of our measurements. The averages were calculated by averaging all measurements within each 1-mm-thick slice of the water column. The wave motion was undiminished at the top of the sublayer, but was not visible nearer the sediments.

To make up the profiles shown (Fig. 1) a steady current was observed for 1 hour. To minimize the effects of waves, the period of highest currents was selected for detailed analysis. At this time the direction of current flow, indicated by a vane, was such that the platform and mounts caused no interference with the flow past the sensors. The averaged full-height profile shows that most of the shear occurred in the lowest centimeter. In the inset of Fig. 1, means of the samples in the 1.2-cm area just above the sediment are shown. The lowest 0.6 cm of these are well fitted by a straight line, indicating viscous flow. The location of the sediment-water interface with respect to the profiles is taken from the zero-velocity height of this line. The shear given by this least-squares fit is 11.9 ± 0.7 sec^{-1} (all error limits are 95 percent confidence estimates). Multiplying this shear by viscosity, $\nu = 0.0150$ g/cm-sec, the value 0.18 ± 0.01 dyne/cm^2 is obtained for the viscous stress. The friction velocity, $u_* \equiv$ (stress/density)$^{1/2}$, is then 0.42 ± 0.012 cm/sec. Above the sublayer the profile is well fitted by a logarithmic form. The drag coefficient, C_D, referred to the (logarithmically) extrapolated 100-cm velocity (12.4 cm/sec) is 0.0011 ± 0.0001, well within the range of previous estimates (*4*), and a little less than the predicted value of 0.0015 for hydrodynamically smooth flow of this speed. The dimensionless height of the sublayer, taken as the height where linear and logarithmic fitted lines meet (Fig. 2) divided by ν/u_*, is 17 ± 1, somewhat larger than the value traditionally given for channel and pipe flow (*5*). One might speculate that these last two effects, that is, the drag coefficient being lower than expected and the dimensionless sublayer thickness being greater, may be a result of the sediment load. In laboratory experiments, sediment added to water has been seen to cause even greater drag reduction and sublayer thickening (*6*).

The energy dissipation in the sublayer, calculated for viscous flow, is 2.12 ± 0.25 erg/cm^3, which becomes 1.27 ± 0.15 erg/cm^2-sec when integrated over the sublayer thickness. Dissipation in the turbulent boundary layer is usually taken to be $C_D \rho U^3$, where ρ is density and U is mean current (taken at 100 cm), so the dissipation in this case is 2.1 erg/

0036-8075/79/0914-1131$00.50/0

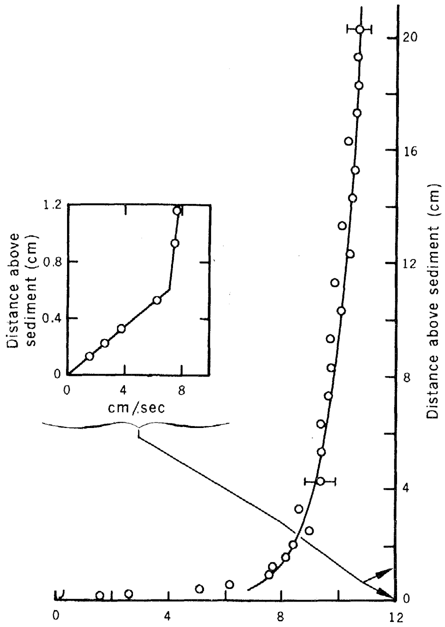

Fig. 1. Average flow speeds plotted against distance above sediment. The curved line in the larger figure and the upper line in the inset represent least-squares fit of a logarithmic form to the speeds above 1 cm. The sloped line in the inset represents a linear fit to the speeds below 0.6 cm. Some 95 percent confidence levels are indicated.

cm^2-sec. This indicates that the dissipation in the sublayer is comparable to that in the rest of the boundary layer, and in fact may well be a large fraction of the energy loss in the entire water column. (This energy when turned into heat is still but a small fraction of the geothermal flux, and so will not have any substantial effect as heat.) It is interesting that Kundu (7) found a comparable energy flux, 1.5 erg/cm^2-sec, being transported to the bottom by inertial-internal waves at a nearby site.

According to the usual arguments in an unstratified, nonrotating turbulent boundary layer

$$\frac{\partial U}{\partial(\log_e Z)} = \frac{u_*}{k}$$

k being the Von Karman constant and Z the distance above the bottom. Combining the value of u_* calculated from sublayer data and the value of the shear in the layer above, one obtains a value of 0.415 ± 0.02 for the Von Karman constant, in remarkable agreement with the 0.41 value usually taken. Fitting the data above the sublayer to the logarithmic form, one obtains a value of 0.00055 cm for the roughness length, Z_0. A roughness Reynolds number $u_* Z_0/\nu$ is then 0.0153, well within the smooth flow regime and consistent with the existence of the viscous sublayer.

Some confirmations of these results are available. A second thermistor on the same traverse produced data in the sublayer, which gave results agreeing within 95 percent confidence limits with the numbers given above. The mean speed indicated by a nonprofiling rotor agreed well (Fig. 2) with the mean speeds calculated from the profiling thermistor. In a wave number spectrum calculated during the period of observation from the rotor data, the energy was seen to fall as (wave number)$^{-5/3}$ for wavelengths from 100 m to 10 m. The spectrum can be interpreted in light of the Ozmidov (8) turbulence model, which predicts a $-5/3$ power law dependence even at length scales at which a true inertial subrange is not likely to exist (9). In this model, a (wave number)$^{-5/3}$ dependence is predicted in wavelength ranges in which there is no significant input of kinetic energy into the system from external forcing. Using this model and the further assumption that there is no significant input of energy at scales smaller than 10 m, a kinetic energy dissipation, ϵ, of 0.013 ± 0.007 erg/cm^3-sec is calculated. Making the usual production-dissipation balance assumptions, $\epsilon = u_*^3/kZ$. Averaging this relation over the rotor height, 20 to 40 cm, we can calculate a u_* from the above value of ϵ. It turns out to be 0.52 ± 0.10, just within its confidence limits of the value calculated in the sublayer.

Stress can be calculated from the available data in three ways: (i) in the sublayer as $\rho\nu(\partial U/\partial Z)$; (ii) from the logarithmic layer as $\rho u_*^2 = \rho(k\ \partial U/\partial \log_e Z)^2$; and (iii) from the rotor spectrum as $\rho u_*^2 = \rho(\epsilon k Z)^{2/3}$. The values calculated, 0.18 ± 0.01, 0.18 ± 0.02, and 0.27 ± 0.10, respectively, are not significantly different. Results of precision comparable to the profile-based calculations are not to be expected from speed spectra.

Obviously not too much is established by one microscale experiment in the ocean, but we have seen here for the first time that the viscous sublayer does exist, and this technique produces good measurements of it. The existence of this viscous sublayer does not necessarily imply a diffusive nature for the transfer of heat and mass. Because the diffusivity of ion species in particular is so much smaller than the viscosity of water, a level of random vertical motion too slow to influence the Reynolds stress, and therefore the shear, could transfer solutes efficiently enough to completely mix this layer. Thus, from flow speed data the effectiveness of the sublayer as a diffusive barrier cannot be assessed. The usual laboratory scaling would imply a diffusive scale of $(D/\nu)^{1/3}$ times the thickness we measure, that is, the diffusive layer would be approximately 10 percent as thick (where D is the species diffusivity). In the real flow, with density gradients and other effects, measurements are required to know whether this relation holds. We will be examining temperature profiles for illumination on this point.

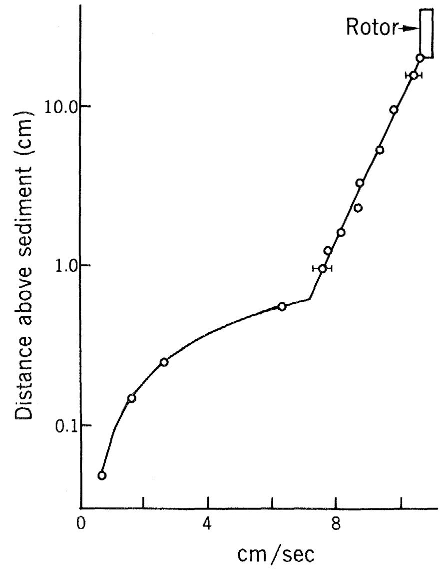

Fig. 2. Average flow speed plotted against distance above sediment. A value derived from a nonprofiling rotor is given. Different averaging was used in making each plot, so the points are not the same.

D. R. CALDWELL
T. M. CHRISS

School of Oceanography,
Oregon State University,
Corvallis 97331

References and Notes

1. I. N. McCave, *The Benthic Boundary Layer* Plenum, New York, 1976); J. C. J. Nihoul, Ed., *Bottom Turbulence* (Elsevier, Amsterdam, 1977); D. J. P. Swift, D. B. Duane, O. H. Pilkey, Eds., *Shelf Sediment Transport* (Dowden, Hutchinson & Ross, Stroudsburg, Pa., 1972); C. M. Gordon, *Nature (London)* **248**, 393 (1974); G. Gust, S. Stolte, *Mar. Geol.* **27**, M1 (1978); D. R. Caldwell, *Rev. Sci. Instrum.* **39**, 1865 (1968); M. H. Wimbush and W. H. Munk, in *The Sea*, A. E. Maxwell, Ed. (Wiley, New York, 1970), vol. 4, part 1, pp. 731-738.
2. E. J. Runge, thesis, Oregon State University (1966).
3. D. L. Inman, *J. Sediment. Petrol.* **22**, 125 (1952).
4. R. W. Sternberg, in *Shelf Sediment Transport*, D. J. P. Swift, D. B. Duane, O. H. Pilkey, Eds. (Dowden, Hutchinson & Ross, Stroudsburg, Pa., 1972), pp. 61-82.
5. J. O. Hinze, *Turbulence* (McGraw-Hill, New York, 1959).
6. G. Gust, *J. Fluid Mech.* **75**, 24 (1976).
7. P. K. Kundu, *J. Phys. Oceanogr.* **6**, 879 (1976).
8. R. V. Ozmidov, *Izv. Acad. Sci. USSR Atmos. Oceanic Phys.* **1**, 257 (1965).
9. T. M. Dillon and T. M. Powell, *J. Geophys. Res.* **81**, 6421 (1976).

10. Financial support was furnished by the Oceanography Section, National Science Foundation, under grant CE77-20242.

5 March 1979; revised 7 May 1979